



Acoustic emission investigation of the mechanical performance of carbon nanotube-modified cement-based mortars



Ilias K. Tragazikis, Konstantinos G. Dassios*, Dimitrios A. Exarchos, Panagiota T. Dalla, Theodore E. Matikas

Department of Materials Science and Engineering, University of Ioannina, Dourouti University Campus, Ioannina GR-45110, Greece

HIGHLIGHTS

- The first AE investigation of CNT-modified cement mortars.
- Air entrapment in matrix overcome by vacuum processing before mixing with the cement.
- Maximum improvements in flexural strength at tube loading of 0.4 wt% of cement.
- Simultaneous maximization of two key AE descriptors at the critical nanotube loading.
- Mortar's fracture mode changes at the critical tube loading, from shear to tensile.

ARTICLE INFO

Article history:

Received 24 November 2015

Received in revised form 14 June 2016

Accepted 20 June 2016

ABSTRACT

Concrete's inherent brittleness, low tensile strength and premature micro-cracking phenomena can be improved by embedment, in the bulk material, of carbon nanotubes (CNT), the 1-D allotrope of carbon exhibiting a remarkable combination of mechanical and transport properties. The present study reports on the flexural and compressive mechanical performance of mortars reinforced with variable loadings of multi-walled carbon nanotubes. Four point bending tests were performed with simultaneous in situ monitoring of the acoustic emission (AE) activity of the mortars, a technique herein applied for the first time in nanotube-reinforced cement, and the data were used to evaluate the efficiency of the non-destructive method in assessing the sensitivity of the mortars' properties on tube loading. A CNT concentration of 0.4% relative to cement mass, was found related to optimal improvements in flexural strength. Impressively, two key AE descriptors, namely average frequency and the rise time over amplitude ratio were independently found to simultaneously maximize at the same tube loading while their temporal variation revealed a transition in the material's fracture mode with tube loading. Complications due air entrapment in the materials facilitated by nanotube presence are discussed in the text and a viable resolution is suggested.

© 2016 Elsevier Ltd. All rights reserved.

1. Introduction

Concrete is the most widely used construction material and great research efforts are continuously invested towards improving its inherent brittleness, low tensile strength and premature micro-cracking behavior by introduction of third phases throughout its volume. While endowment of reinforcement and ductility are conventionally achieved through embedment of steel rods, complementary reinforcement of the continuous phase can be achieved by introduction of other micro- and nano-scale media [1,2].

Nanotechnology currently plays a leading role towards this end. Therein, concrete's properties can be improved by addition of

nanomaterials such as carbon nanotubes (CNTs) [3], the revolutionary one-dimensional allotrope of carbon with Young's moduli approaching 1.4 TPa, seven times higher than of high-strength steel and tensile strengths above 100 GPa, fifty times higher than the same reference material. CNT-based nanocomposites are currently been considered as the next generation materials for aeronautical, electronics, medicine, civil engineering and other applications [4,5]. Carbon nanotubes synthesized by chemical vapor deposition (CVD) and its variants (low pressure-, thermal-, catalytic- and others) have minimum diameters of 0.4 nm and are classified as single- or multi-walled (SWCNTs and MWCNTs, respectively), depending on the number of concentric graphene cylinders that comprise their shell. The latter type, with mechanical, electrical and thermal transport performances only slightly inferior to costly SWCNTs, is the most popular and affordable choice due to their ease of fabrication and low commercial price.

* Corresponding author.

E-mail address: kdassios@cc.uoi.gr (K.G. Dassios).

Investigation of their efficiency as primary reinforcing materials in a variety of contemporary nano-reinforcement applications including construction materials, is currently a leading scientific trend [6]. Carbon nanofibers (CNFs), a similar nanostructured material comprised of cylindrically-shaped arrangements of stacked graphene plates or cones, have also been suggested as nano-reinforcements for concrete [7,8].

Today, two of the most challenging tasks in the emerging field of CNT-reinforced concrete is the achievement of homogeneous dispersion of tubes within the continuous phase and the establishment of proper interfacial bonding which will enable efficient load transfer from the cement matrix to the tubes. These tasks attract rigorous scientific efforts due to the inherent tendency of CNTs to agglomerate due to their high surface area and the strong Van der Waals forces acting between them. The agglomerates are responsible not only for stress concentration within the cement matrix which leads to strength degradation during service life, but also to premature crack initiation. Effective MWCNT dispersion, ideally without significant reduction in the tubes' high initial length and aspect ratio, is currently an open challenge in nanocomposite fabrication and is usually achieved through the use of surfactants [8–10]. Such usage is not always without side-effects. For example, Yazdanbakhsh [8] reported incompatibility issues, during the hydration phase, between cement base and the surfactants used for improving CNT dispersion; the study also observed MWCNT length deterioration and aspect ratio impairment during exposure of the tubes to the high sonication energies required for their disentanglement. It was suggested that the favorable dispersion characteristics achievable in aqueous environments do not guarantee similarly favorable dispersion within the cement matrix. In one of the limited studies available on the CNT-cement interface, Makar et al. reported strong early-age bonds between cement paste and CNTs [11].

Enhancement of cement's compressive and flexural strengths by CNTs has been investigated by a number of researchers and a wide variety of improvements have been reported. Bharj et al. [12] showed a 22% increase in the primer strength by addition of 0.1 wt% MWCNTs. The same property was found increased by 30% by Kim et al. [13], at 0.15 wt% MWCNT loading. Collins et al. [14] found that 0.5 wt% of MWCNTs can increase the concrete's compressive strength by 25%. Musso et al. [15] investigated the effect of pristine annealed and carboxy-group functionalized MWCNTs, 0.5 wt% loadings, on the compressive and flexural strengths of cement nanocomposites, and found the properties increased by 10–20% and 34%, respectively, compared to pure cement. Cwirzen et al. [16] found that addition of only 0.045–0.15 wt% of MWCNT to cement paste can increase its compressive and flexural strengths by 50% and 25% respectively. Nasibulina et al. [17] reported a record 300% increase in compressive strength achieved with 0.4 wt% CNFs. Improvements of the same property by 42.7% and 21.4% were reported by Gao et al. for additions of 0.16 wt% and 1 vol% CNF, respectively [18,19]. Sobolkina et al. [20] reported that the compressive strength of cement paste did not improve for CNT loadings up to 0.05 wt% of cement. Kariene et al. [21] showed that addition of 0.02 wt% of MWCNTs in cement paste can lead to an increase in compressive strength by 11.03% while addition of 0.004 wt% MWCNTs lead to an increase in flexural strength by 11.23%. Camacho [9] reported that MWCNT addition to Portland cement mortars does not significantly affect mechanical properties at 28 days curing time; he found increases smaller than 6% and 7% in bending and compressive strength, respectively.

Interaction between CNTs and the continuous bulk phase is a topic of particular relevance in nano-reinforced cement. Nochaiya and Chaipanich [22] found that addition, up to 1 wt% of cement, of CVD-prone MWCNTs synthesized with nickel oxide as catalyst,

ensures a dense microstructure as a result of the tubes acting as filler for concrete voids; at the same time a strong tube-matrix bond leads to increased strength. Similar results were independently reported by Chaipanich et al. for CNT-reinforced fly ash-cement matrices [23]. Sobolkina et al. investigated the effects of two different surfactants, SDS and Brij 35, on CNT dispersion efficiency and the mechanical properties of cement matrix. SDS was found associated with severe strength drops of hardened cement due to foam formation leading to introduction of porosity in the cement paste while Brij 35 presence had no influence on strength and porosity [24]. Camacho found that the addition of CNTs to Portland cement mortars does not significantly affect the apparent density, after 28 days of curing period. Concerning porosity, only slight increases could be detected after the same period in CNT-cement mortars. Such increases could signify development of corrosion in aggressive conditions, such as carbonation and contamination by chloride ions.

In the present study, the compressive and flexural strengths of mortars reinforced with varying concentrations of carbon nanotubes are measured with simultaneous in situ monitoring of the acoustic emission activity of the material with aim not only to benchmark the non-destructive technique across nanotube-reinforced cement-based materials -which to the authors' knowledge is herein applied for the first time to such media- but also to investigate the relation between nanotube loading and the microstructure of the material, and establish the optimal tube concentration for maximization of the mechanical performance. The efficiency of acoustic emission in accurately assessing the mechanical properties' sensitivity to nanotube loading is also benchmarked together with the potential of the technique in following the fracture mode in real testing time. The role and importance of key AE descriptors is discussed in the text.

2. Materials and methods

2.1. Materials, specimens and testing

The MWCNTs used in the present work were synthesized via catalytic chemical vapor deposition and were commercially available by Shenzhen Nanotech Port Co. Ltd. (Shenzhen, China). Their nominal purity was higher than 97% and their amorphous carbon content less than 3%. Nominal tube diameter ranged from 20 to 40 nm while their length ranged from 5 to 15 μm . Viscocrete Ultra 300 (Sika AG, Baar, Switzerland), a water-based superplasticizer comprised of polycarboxylate polymers was used as dispersion assistive agent; it was selected based on its efficiency in inhibiting air entrapment inside the specimens as well as because of its excellent resistance to mechanical and chemical attack.

For the production of cement/CNT mixtures with tube loadings variable within 0.2, 0.4, 0.5, 0.6 and 0.8 wt% of cement, the following experimental protocol was adopted. Initially, aqueous suspensions of MWCNTs were prepared by mixing, under magnetic stirring for 2 min, of the superplasticizer and tubes at a ratio of 1.5/1, in regular tap water. The resultant suspensions were subsequently ultrasonicated for 90 min at room temperature by aid of a Hielscher UP400S device (Hielscher Ultrasonics GmbH, Teltow, Germany) equipped with a cylindrical 22 mm diameter sonotrode delivering a power throughput of 4500 J/min at a frequency of 24 kHz. The specific combination of ultrasonication parameters was established as optimal for achievement of suspension homogeneity without tube aspect ratio impairment following a tedious parametric study which involved CNT agglomerate size analysis as a function of ultrasonication duration and energy [10].

The ultrasonicated suspensions were transferred, along with ordinary Portland cement type "I 42.5N" and natural sand into the bucket of a rotary mixer where they were mixed for a total of 4 min, in low and high speeds sequentially, as per standard test method BS EN 196-1. Immediately after mixing, the fresh mortar was poured into metallic oiled formworks, volumes of $160 \times 40 \times 40 \text{ mm}^3$, where it was left for 24 h before demolding and subsequent placement into a 100% humidity room for a duration of 28 days. A total 60 specimens were prepared, divided into two sets of six specimens at each CNT formulation, 0.2, 0.4, 0.5, 0.6 and 0.8 wt% of cement. In one set, suspensions were further processed in a vacuum environment for removal of entrapped air before they were mixed with the cement and sand by aid of a rotary mixer. Additional mixtures without nanotubes were also prepared for reference purposes. Fig. 1 depicts the as-processed state of MWCNT-reinforced concrete specimens with varying tube loadings. The bottom row depicts reference

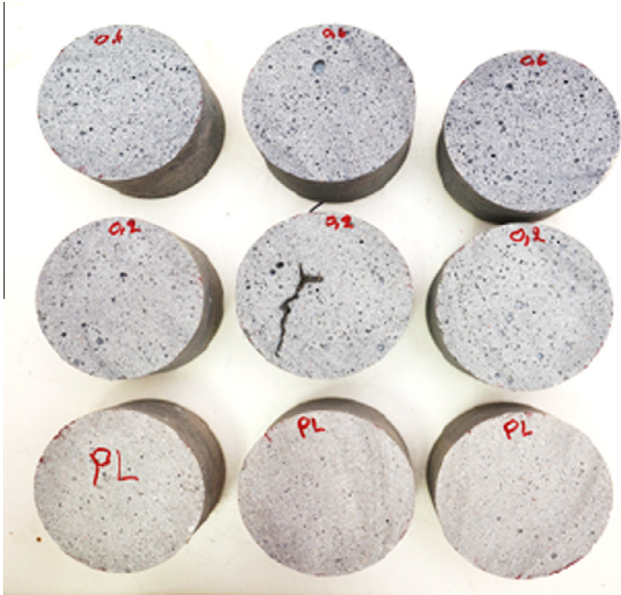


Fig. 1. As-processed cement specimens with various amounts of carbon nanotube loadings: 0.6 wt% of cement (top row), 0.2 wt% of cement (middle row) and plain cement (bottom row).

specimens, whereas the top and middle rows show specimens with tube loadings of 0.6 and 0.2 wt% of cement, respectively, wherein porosity appears to increase with nano-reinforcement concentration.

Mechanical characterization under four point bending testing configuration according to standard test protocol ASTM C1609 was performed on an Instron 5967 testing frame (Instron, Norwood, MA, USA) equipped with a 30 kN loadcell. Compression testing at a load rate of 2400 N/s, which corresponds to a stress rate of 1.5 MPa/s for the $40 \times 40 \text{ mm}^3$ tested area, was performed following standard protocol EN 196-1:2005.

2.2. Acoustic emission monitoring

Acoustic emission is widely used for monitoring damage accumulation in concrete structures; the operating principle of the technique relies on the rapid release of acoustic energy from different localized sources inside a material which generate elastic waves due to damage creation and evolution [23]. Such waves propagate through the solid and the amount of acoustic energy released depends on the size and the speed of the local deformation process and on the nature of the material. AE can detect and monitor deformation, crack formation and growth and corrosion damage in concrete structures. The transducers are usually piezoelectric and transform the energy of the transient elastic wave to an electric waveform which is digitized and stored. AE sensors record the accumulated activity which is indicative of the severity of damage. Specific descriptors relating to the magnitude or population of AE signals have been successfully suggested for monitoring the health of

heterogeneous structural materials such as concrete and composites [25–27]. Simultaneous usage of multiple sensors facilitates location of source events based on the time delay recorded between acquisitions of corresponding signals at the different sensor sites. This allows identification of the material section requiring repair, a task which is of paramount importance for large-scale structures. AE data can also reveal the mode of fracture of a material [27,28].

A number of AE parameters can be defined in a typical AE waveform, Fig. 2. Amplitude (A) is the maximum voltage of the AE signal and is measured in decibels (dB), threshold is a user defined amplitude value in dB based on background noise level, rise time (RT) is the time between the first threshold crossing and maximum peak amplitude. RA is a key AE parameter defined as the ratio of rise time over amplitude (RT/A). AE counts are the number of times an AE burst crosses the threshold, AE duration is the time between the first and last threshold crossing and AE energy is the area under the amplitude–time curve above the threshold value.

Other important AE aspects are based on qualitative parameters of received signals. Primarily, the shape of the waveform is indicative of the fracture type, information which is very important for the classification of cracks in different materials. As shear cracks appear first during damage accumulation in the material and tensile ones appear next, characterization of the cracking mode can act as a warning against final failure. Additionally, tensile events are linked to higher frequency content and higher RA values, than shear events [29–32]. This is mainly due to the larger part of energy transmitted in the form of shear waves which are slower than longitudinal one and therefore the maximum peak of the waveform delays are compared to the onset of the initial longitudinal arrivals [2,33]. This kind of classification has proven useful in laboratory conditions concerning corrosion cracking in concrete [29], fracture of cross-ply laminates [30,31], as well as discrimination between tensile matrix cracking and fiber pull-out during bending of steel-fiber reinforced concrete [32]. Finally, average frequency (AF, kHz), defined as the number of counts divided by the duration of the signal, has been suggested for the characterization of the cracking mode of the material, with shifts from higher to lower values indicating a correspondent shift in cracking mode from tensile to shear [2,29,33,34].

AE activity was monitored on four point bending tests of MWCNT-reinforced concrete specimens in real testing time using two R15a AE sensors (Physical Acoustics Corp, Princeton, New Jersey, USA), with broadband response ranging from 50 to 400 kHz and a maximum sensitivity at 150 kHz, attached on the lower section of the specimen. The R15a is a high-sensitivity narrow band resonant sensor. The pre-amplifier gain was set at 40 dB and the signals were recorded on a dedicated PCI-2 board (Physical Acoustics Corp, Princeton, New Jersey, USA). To exclude possible noise recording, the threshold was set at 45 dB. The sensors were attached on one side of the specimen at a distance of 40 mm.

3. Results and discussion

3.1. Mechanical performance

The effect of CNT loading on the flexural and compressive strengths of investigated concretes is summarized in Table 1 and Fig. 3. It is primarily observed that subsection of the suspension to the vacuum-assisted air removal procedure significantly enhanced the material's flexural strength, compared to non-vacuumed suspensions. Specimens originating from non-vacuumed suspensions, exhibited flexural strengths under four

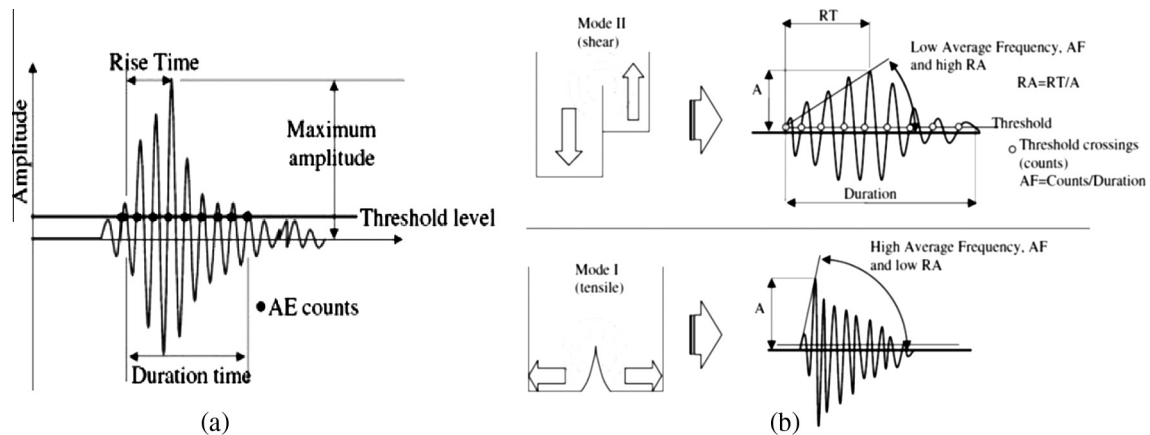


Fig. 2. a. Typical AE signal and definition of related parameters. b. Typical AE signals due to different type of fracture.

Table 1
Flexural and compressive strength of MWCNT-reinforced concrete.

CNT loading, wt% of cement	Flexural Strength [MPa]		Compressive Strength [MPa]	
	Non-vacuumed suspensions	Vacuumed suspensions	Non-vacuumed suspensions	Vacuumed suspensions
0 (plain)	5.36 ± 0.38	5.43 ± 0.23	63.75 ± 2.43	67.84 ± 1.91
0.2	4.15 ± 0.28	6.09 ± 0.43	71.68 ± 1.68	67.94 ± 2.03
0.4	4.61 ± 0.48	6.34 ± 0.67	66.3 ± 4.38	66.73 ± 3.18
0.5	4.45 ± 0.21	5.93 ± 0.84	61.91 ± 5.49	67.04 ± 2.43
0.6	4.97 ± 0.36	6.01 ± 0.66	65.43 ± 3.71	66.81 ± 2.7
0.8	4.78 ± 0.21	5.92 ± 0.5	65.4 ± 1.51	70.37 ± 2.11

point bending which were systematically lower not only from their vacuumed counterparts, but also from control values. This behavior is attributed to nanotube presence facilitating – in a superplasticizer-rich environment – air entrapment in the mortar matrix. Additionally, strength did not vary monotonically with increasing tube loading, a behavior which is not unlinked to the high porosity of specimens of non-vacuumed suspensions. As depicted in Fig. 1, the flexural strength of specimens of vacuumed suspensions, appeared to increase with increasing tube content up to 0.4 wt% cement. Above that threshold, the property decreases with nanotube loading with values remaining nonetheless higher than those of reference specimens. This behavior constitutes a well-established characteristic of nanotube-reinforced matter and can be rationalized upon nanotube agglomeration at higher loading fractions which severely inhibits material properties by introduction of defect locations such as air cavities, porosity, incomplete interfacial bonding and matrix-stagnant areas in the otherwise continuous medium [10]. For vacuumed suspensions, the maximum improvement in flexural strength compared to

control specimens, appeared at 0.4 wt% MWCNT loading and was approximately 17%; respective improvements at loadings of 0.2, 0.5, 0.6 and 0.8 wt% were 12, 9, 10 and 9%. The observed confinement of mechanical property improvements below a certain reinforcement loading threshold is in accordance with previous reports. Soulioti et al. found mechanical property improvements in steel-fiber reinforced concrete similarly limited to loadings below 1.5 wt%; property deterioration was reported at higher loadings.

In terms of compressive strength, no substantial change in the property was observed for vacuumed specimens within the investigated range of MWCNT loading. The maximum increase, a marginal 3%, was noted for the highest tube loading, 0.8 wt% of cement. Compressive strength followed an unconventional zig-zag trend for non-vacuumed suspensions as observed in Fig. 3. Interestingly, strength variation remained within 10% for the two types of suspensions throughout the entire tube loading range.

3.2. Acoustic emission monitoring

The average values of acoustic emission activity and energy are depicted in Fig. 4 as functions of varying MWCNT composition in the cement matrix, for both vacuumed and non-vacuumed suspensions. For the primer materials, the amount of acoustic activity is observed to increase with increasing tube loading with the mean AE hits value in specimens with 0.8 wt% CNTs found 30 times more than in plain specimens. The trend of increasing AE activity with nanotube loading noted in Fig. 4 is due to the splitting, at MWCNT locations, of the macrocracks propagating throughout the matrix under the bending moment. This multiple microcrack generation and crack deflection is more intense as the possible split locations increase in number with increasing nanotube loading, which leads

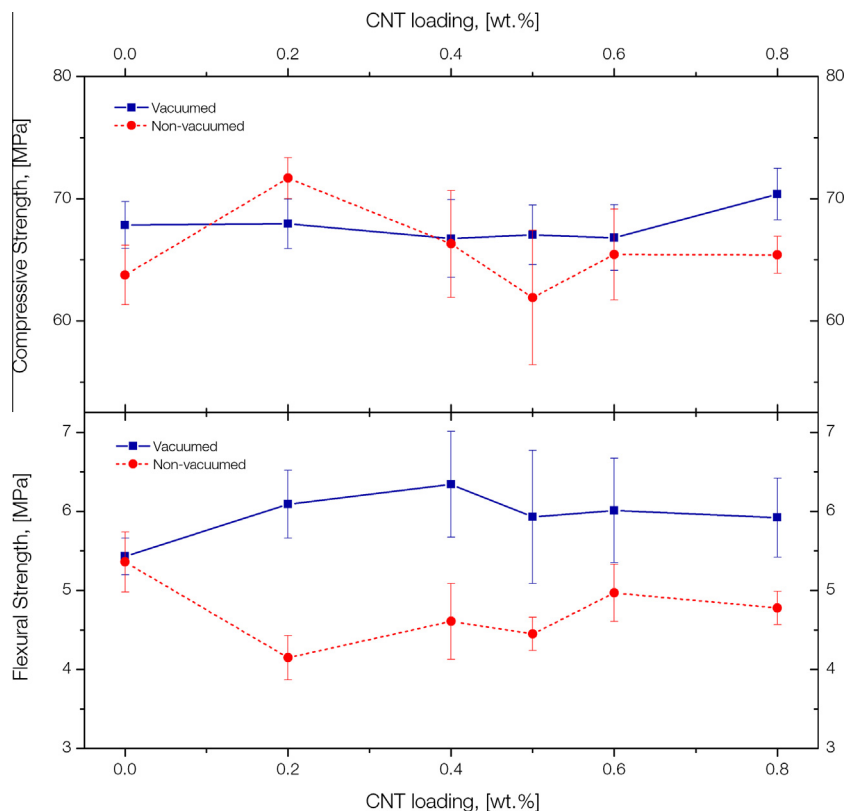


Fig. 3. Variation of flexural strength (top) and compressive strength (bottom) of MWCNT-reinforced mortars as a function of tube loading for vacuumed and non-vacuumed suspensions.

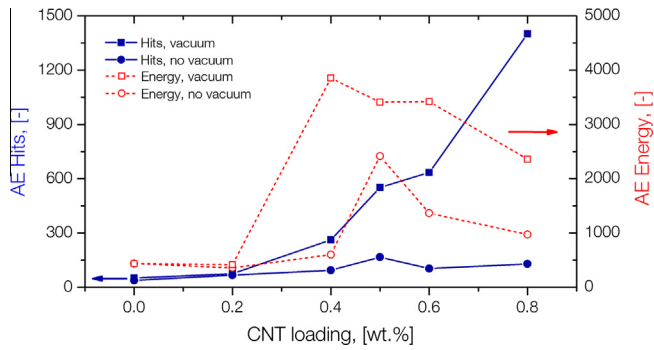


Fig. 4. Average AE hits and energy during four point bending tests of mortars reinforced with variable loadings of MWCNTs.

to a greater acoustic emission activity. This particular AE activity pattern is similar to previous reports in the literature for steel-fiber reinforced concrete under bending [2]. In contrast to their vacuumed counterparts, the acoustic emission activity of specimens of non-vacuumed suspensions, appeared to increase negligibly with tube loading. This behavior is linked to the introduction of porosity and entrapment of air in the originating non-vacuumed suspensions which lead to an overall weakened mechanical performance, even lower than reference values, wherein the exact nanotube loading, hence also its AE activity potential, were of small importance. In other words, increased porosity had severely adverse effects on the matrix and consequently also to AE activity.

A separate acoustic emission descriptor, namely AE energy or the amount of energy released during the 4-point bending test, was observed to be highest for samples loaded with 0.4 wt% MWCNTs. This finding indicates that the energy released during bending by the specimens due to micro-cracking processes was higher than the energy of more concentrated specimens, despite the fact that mere hit count was higher in the latter case. Most interestingly, the nanotube concentration found, herein, associated with the release of the maximum AE energy, 0.4 wt%, coincides with the value previously found related to the greatest improvement in flexural strength. This particular finding indicates that the AE technique can independently validate and assess the effect of tube presence on the mechanical performance of the nano-reinforced mortars. Comparing the acoustic emission activities between specimens originating from vacuumed and non-vacuumed suspensions, a 5-fold increase is noted in the primer mortars compared to the latter. The relation between AE energy and the fracture energy of cement-based materials has been highlighted in the literature [35–37]. A systematic experimental study is currently under way for the establishment of the correlation between variable nanotube loading and acoustic emission energy as a quantitative measure for characterizing the fracture energy in MWCNT-reinforced mortars.

Average RA is plotted as a function of MWCNT concentration in the cement matrix in Fig. 5. It is observed that addition of MWCNTs up to 0.4 wt%, leads to considerable increase in RA. In four point bending tests, where crack formation is localized at the bottom horizontal plane where shear stresses concentrate, higher RA values indicate shear fracture wherein cracks initiating under the action of tension, eventually propagate under the shear stresses which take over the failure process [2]. This also explains the experimental observation that specimen failure did not occur under a single vertical macrocrack but followed a multiple cracking pattern, with significant crack deflection, at tube loadings above 0.4 wt% of cement. Interestingly and consistently with previous observations, the highest RA value is recorded at a concentration of 0.4%, the same value previously found related to both maximum

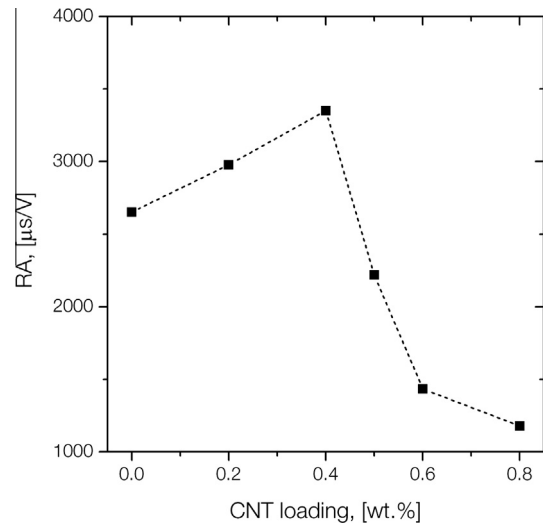


Fig. 5. Variation of the average RA value as a function of MWCNT concentration in the mortars.

AE energy and maximum flexural strength improvement. Further increase in tube loading above the 0.4 wt% threshold, results in a decrease in RA at values lower than control specimens.

Based on previous observations by Soulioti et al. that shear and tensile fracture modes are linked to specific AF and RA values [2], the sensitivity of acoustic emission data on failure mode can be exclamationed by plotting the variations of RA and AF against four point bending test duration, for three selected nanotube loadings, namely 0 (plain), 0.4 and 0.8 wt%, as shown in Fig. 6. It is observed that RA varies around an average value of ca. 4000 $\mu\text{s}/\text{V}$ for plain specimens while the property decreases to approximately 2000 $\mu\text{s}/\text{V}$ for 0.8% loaded specimens. In the same range, AF increases from ca. 35 to ca. 50 kHz. The 35 kHz AF value of plain specimens suggests a shear failure mode whereas the 50 kHz value is close to the 60 kHz literature value indicating tensile failure [2]. In the same context, RA values above 4000 $\mu\text{s}/\text{V}$ indicate a shear fracture mode while values near 2000 $\mu\text{s}/\text{V}$ indicate a tensile one. Based on the above argumentation, it is concluded that the acoustic emission technique can autonomously assess and report the fracture mode of CNT-modified mortars and eventual transitions between various modes.

4. Conclusions

The present paper reports on the flexural and compressive mechanical performance of CNT-reinforced mortars, at tube loadings variable within 0–0.8 wt%, tested under compression and four point bending with real time AE monitoring in the latter tests. It was found that nanotube presence facilitates air entrapment inside the matrix which, in turn, can lead to decreased mechanical performance of the mortars. The complication was overcome by submitting the nanotube suspension to vacuum processing before mixing with the cement. The maximum improvements in flexural strength were noted at a tube loading of 0.4 wt% of cement; above this threshold property values decreased with tube loading, remaining in all cases higher, by 10%, than control values. Compressive strength was found practically invariant within the investigated tube loading range. In situ-captured acoustic emission data revealed simultaneous maximization of two key AE descriptors, namely released AE energy and rise time over amplitude ratio (RA value), at the critical nanotube loading value of 0.4 wt%. The variation, with tube loading, of the AF descriptor revealed an

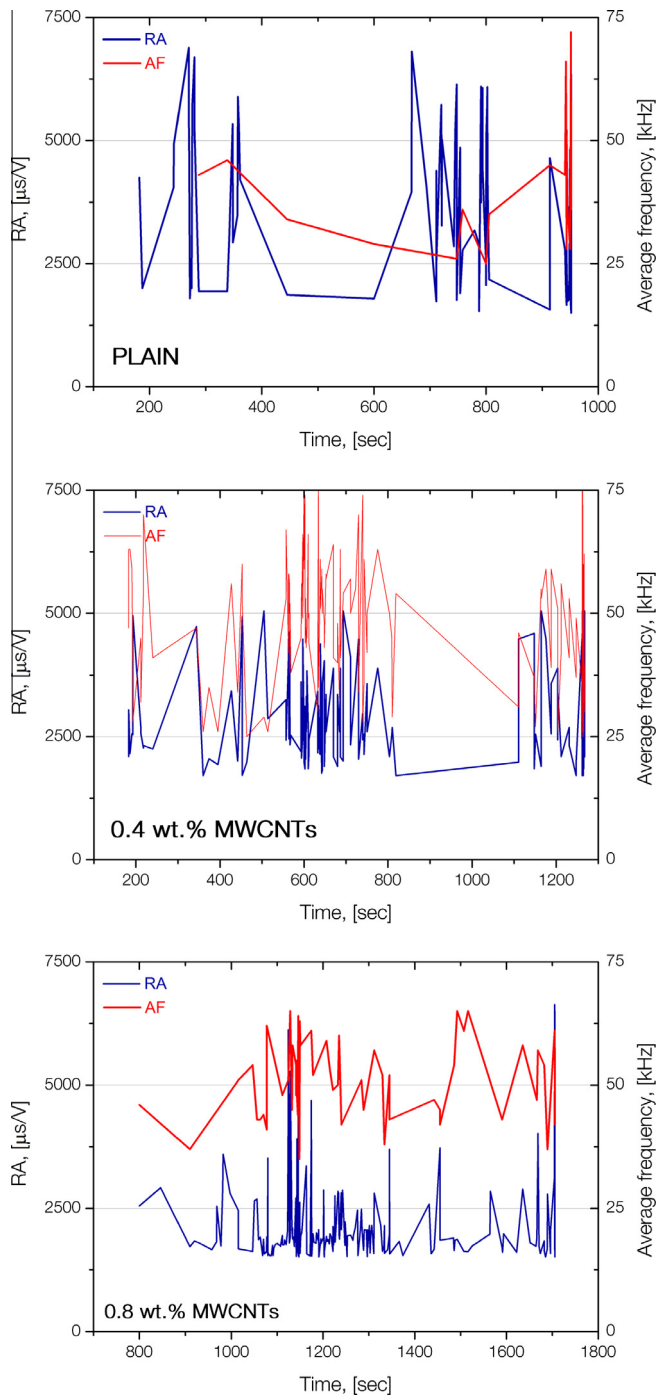


Fig. 6. Temporal variations of average RA and AF in three mortars with variable CNT loadings.

impressive transition, at the same tube concentration, of the mortars' fracture mode from shear to tensile. These observations benchmark the AE technique as completely autonomous in assessing the mechanical and fracture performance of nano-modified mortars.

Acknowledgments

This research project has been cofinanced by the European Union (European Regional Development Fund – ERDF) and Greek national funds (General Secretariat for Research and Technology) through the Operational Program “Competitiveness and

Entrepreneurship and Regions in Transition” of the National Strategic Reference Framework (NSRF 2007–2013), under the program “Cooperation 2011, Partnerships of Production and Research Institutions in Focused Research and Technology Sectors”.

References

- [1] R.K. Abu Al-Rub, A.I. Ashour, B.M. Tyson, On the aspect ratio effect of multi-walled carbon nanotube reinforcements on the mechanical properties of cementitious nanocomposites, *Constr. Build. Mater.* 35 (2012) 647–655.
- [2] D. Soulioti, N.M. Barkoula, A. Paipetis, et al., Acoustic emission behavior of steel fibre reinforced concrete under bending, *Constr. Build. Mater.* 23 (12) (2009) 3532–3536.
- [3] S. Iijima, Helical microtubules of graphitic carbon, *Nature* 354 (6348) (1991) 56–58.
- [4] M.-F. Yu, O. Lourie, M.J. Dyer, et al., Strength and breaking mechanism of multiwalled carbon nanotubes under tensile load, *Science* 287 (5453) (2000) 637–640.
- [5] B. Peng, M. Locascio, P. Zapol, et al., Measurements of near-ultimate strength for multiwalled carbon nanotubes and irradiation-induced crosslinking improvements, *Nat. Nanotechnol.* 3 (10) (2008) 626–631.
- [6] R. Siddique, A. Mehta, Effect of carbon nanotubes on properties of cement mortars, *Constr. Build. Mater.* 50 (2014) 116–129.
- [7] J.P. Salvetat, J.M. Bonard, N.H. Thomson, et al., Mechanical properties of carbon nanotubes, *Appl. Phys. A* 69 (3) (1999) 255–260.
- [8] A. Yazdanbakhsh, Z. Grasley, B. Tyson, et al., Distribution of carbon nanofibers and nanotubes in cementitious composites, *Trans. Res. Rec. J. Trans. Res. Board* 2142 (1) (2010) 89–95.
- [9] M. del Carmen Camacho, O. Galao, F. Baeza, et al., Mechanical properties and durability of CNT cement composites, *Materials* 7 (3) (2014) 1640–1651.
- [10] K.G. Dassios, P. Alafogianni, S.K. Antiohos, et al., Optimization of sonication parameters for homogeneous surfactant-assisted dispersion of multiwalled carbon nanotubes in aqueous solutions, *J. Phys. Chem. C* 119 (13) (2015) 7506–7516.
- [11] J. Makar, J. Margeson, J. Luh, Carbon nanotube/cement composites – early results and potential applications, 3rd International Conference on Construction Materials: Performance, Innovations and Structural Implications (2005) 1–10.
- [12] J. Bharj, S. Singh, S. Chander, et al., Experimental study on compressive strength of Cement-CNT composite paste, *Indian J. Pure Appl. Phys.* 52 (1) (2014) 35–38.
- [13] H.K. Kim, I.W. Nam, H.K. Lee, Enhanced effect of carbon nanotube on mechanical and electrical properties of cement composites by incorporation of silica fume, *Compos. Struct.* 107 (2014) 60–69.
- [14] F. Collins, J. Lambert, W.H. Duan, The influences of admixtures on the dispersion, workability, and strength of carbon nanotube–OPC paste mixtures, *Cement Concr. Compos.* 34 (2) (2012) 201–207.
- [15] S. Musso, J.-M. Tulliani, G. Ferro, et al., Influence of carbon nanotubes structure on the mechanical behavior of cement composites, *Compos. Sci. Technol.* 69 (11–12) (2009) 1985–1990.
- [16] A. Cwirzen, K. Habermehl-Cwirzen, V. Pentala, Surface decoration of carbon nanotubes and mechanical properties of cement/carbon nanotube composites, *Adv. Cem. Res.* 20 (2) (2008) 65–73.
- [17] L.L. Nasibulina, I.V. Anoshkin, A.V. Semencha, et al., Carbon nanofiber/clinker hybrid material as a highly efficient modifier of mortar mechanical properties, *Mater. Phys. Mech.* 13 (1) (2012) 77–84.
- [18] D. Gao, M. Sturm, Y.L. Mo, Electrical resistance of carbon-nanofiber concrete, *Smart Mater. Struct.* 18 (9) (2009) 95039–95045.
- [19] B. Han, S. Sun, S. Ding, et al., Review of nanocarbon-engineered multifunctional cementitious composites, *Compos. A Appl. Sci. Manuf.* 70 (2015) 69–81.
- [20] A. Sobolkin, V. Mechtcherine, V. Khavrus, et al., Dispersion of carbon nanotubes and its influence on the mechanical properties of the cement matrix, *Cement Concr. Compos.* 34 (10) (2012) 1104–1113.
- [21] J. Kerienė, M. Kligys, A. Laukaitis, et al., The influence of multi-walled carbon nanotubes additive on properties of non-autoclaved and autoclaved aerated concretes, *Constr. Build. Mater.* 49 (2013) 527–535.
- [22] T. Nochaiya, A. Chaipanich, Behavior of multi-walled carbon nanotubes on the porosity and microstructure of cement-based materials, *Appl. Surf. Sci.* 257 (6) (2011) 1941–1945.
- [23] A. Chaipanich, T. Nochaiya, W. Wongkeo, et al., Compressive strength and microstructure of carbon nanotubes–fly ash cement composites, *Mater. Sci. Eng., A* 527 (4–5) (2010) 1063–1067.
- [24] A. Sobolkin, V. Mechtcherine, V. Khavrus, et al., Dispersion of carbon nanotubes and its influence on the mechanical properties of the cement matrix, *Cement Concr. Compos.* 34 (10) (2012) 1104–1113.
- [25] J.H. Kurz, F. Finck, C.U. Grosse, et al., Stress drop and stress redistribution in concrete quantified over time by the b-value analysis, *Struct. Health Monit.* 5 (1) (2006) 69–81.
- [26] D.G. Aggelis, T. Shiotani, S. Momoki, A. Hiram, Acoustic emission and ultrasound for damage characterization of concrete elements, *Mater. J.* 106 (6) (2009).
- [27] C. Grosse, H. Reinhardt, T. Dahm, Localization and classification of fracture types in concrete with quantitative acoustic emission measurement techniques, *NDT and E Int.* 30 (4) (1997) 223–230.

- [28] T.K. Haneef, K. Kumari, C.K. Mukhopadhyay, et al., Influence of fly ash and curing on cracking behavior of concrete by acoustic emission technique, *Constr. Build. Mater.* 44 (2013) 342–350.
- [29] Y. Tomoda, M. Ohtsu, Phenomenological model of corrosion process in reinforced concrete identified by acoustic emission, *Mater. J.* 105 (2) (2011).
- [30] Y. Mizutani, K. Nagashima, M. Takemoto, et al., Fracture mechanism characterization of cross-ply carbon-fiber composites using acoustic emission analysis, *NDT E Int.* 33 (2) (2000) 101–110.
- [31] D.G. Aggelis, N.M. Barkoula, T.E. Matikas, Acoustic emission monitoring of degradation of cross ply laminates, *J. Acoust. Soc. Am.* 127 (6) (2010) EL246–EL251.
- [32] D.G. Aggelis, D.V. Soulioti, N. Sapouridis, et al., Acoustic emission characterization of the fracture process in fibre reinforced concrete, *Constr. Build. Mater.* 25 (11) (2011) 4126–4131.
- [33] T. Shiotani, M. Ohtsu, K. Ikeda, Detection and evaluation of AE waves due to rock deformation, *Constr. Build. Mater.* 15 (5–6) (2001) 235–246.
- [34] Recommendation of RILEM TC 212-ACD: acoustic emission and related NDE techniques for crack detection and damage evaluation in concrete*, *Mater. Struct.* 43 (9) (2010) 1183–1186.
- [35] R. Vidya Sagar, B.K. Raghu Prasad, An experimental study on acoustic emission energy as a quantitative measure of size independent specific fracture energy of concrete beams, *Constr. Build. Mater.* 25 (5) (2011) 2349–2357.
- [36] S.P. Shah, *Fracture Toughness of Cement-Based Materials*, Springer, New York, NY, 1989.
- [37] E.N. Landis, L. Baillon, Acoustic emission measurements of fracture energy, *Fract. Mech. Concr. Struct.* 1 (2001) 389–394.